American Mineralogist, Volume 68, pages 972–980, 1983

A review of the todorokite–buserite problem: implications to the mineralogy of marine manganese nodules

ROGER G. BURNS, VIRGINIA MEE BURNS AND HARLAN W. STOCKMAN[1]

Department of Earth and Planetary Sciences
Massachusetts Institute of Technology
Cambridge Massachusetts 02139

Abstract

The names todorokite and buserite are two competing terminologies for the abundant manganese oxide mineral occurring in deep-sea manganese nodule deposits. Proponents of the buserite phase claim it to be the parent of todorokite which is considered to be a mixture of buserite and its breakdown products birnessite and manganite (γ-MnOOH). The recent experimental evidence demonstrating the integrity of todorokite (a tekto-manganate with multidimensional tunnels formed by walls of edge-shared [MnO_6] octahedra) has led to an assessment of the proposed relationships between synthetic buserite (a phyllo-manganate containing layers of edge-shared [MnO_6] octahedra) and its transformation products. Inconsistencies are found to exist in published electron diffraction data underlying the proposed topotactic transformation mechanism of synthetic birnessite platelets to acicular "γ-MnOOH" crystallites suggested to constitute natural todorokites. The crystal chemistry of todorokite structure-types is discussed. We suggest that three types of atomic substitution occur in the tunnel structures: first, substitution of Mn^{2+} by other divalent cations (*e.g.*, Mg^{2+}, Ni^{2+}, Cu^{2+}, Zn^{2+}) in the "walls" formed by chains of edge-shared [MnO_6] octahedra, characteristically three octahedra wide; second, replacement of Mn^{4+} by similar sized cations (*e.g.*, low-spin Co^{3+}) in the "ceilings" or "floors" typically three, but as many as seven or more, [MnO_6] octahedra wide; and third, in the tunnel interiors adjacent to Mn^{4+} vacancies in the "ceilings." Here, a variety of large cations (K^+, Ba^{2+}, Ag^+, Pb^{2+}, Ca^{2+}, Na^+), H_2O molecules, and hydrated transition metal cations could be accommodated. We recommend that the name todorokite be universally adopted for the predominant manganese oxide mineral accommodating divalent cations of nickel and copper in marine manganiferous concretions.

Introduction

One of the most common manganese oxide phases detected in marine ferromanganese nodules, crusts and metalliferous sediments is that with characteristic X-ray diffraction lines at 9.5–9.8Å and 4.8–4.9Å. Chemical and electron microprobe analyses of this nodule 10Å phase phase indicate that it is a hydrated Mn–Mg–Ca–Na–Ni–Cu oxide. Its ability to concentrate Ni and Cu to several weight percent (Burns and Burns, 1978, 1979b) makes deep-sea manganese nodules the focus of considerable scientific and economic interest (Glasby, 1977; Cronan, 1980).

X-ray diffraction patterns similar to that of the nodule 10Å phase are shown by two other species: todorokite, a Mn–Mg–Ca–Na–K oxide originally reported in a non-marine environment (Yoshimura, 1934); and derivatives of a synthetic sodium manganese oxide hydrate (Feitknecht and Marti, 1945; Wadsley, 1950a, b) called "10Å manganite." As a result, the phase occurring in manganese nodules was identified as either todorokite (Straczek *et al.*, 1960; Hewitt *et al.*, 1963), or synthetic "10Å manganite" (Buser, 1959). This dual nomenclature has pervaded the literature on marine manganese deposits (Burns and Burns, 1977a, 1979b), despite the complaint (Arrhenius, 1963) that the term "10Å manganite" causes confusion with the mineral manganite (γ-$Mn^{III}OOH$).

Giovanoli *et al.* (1971) proposed that the nodule 10Å phase be called buserite, in honor of W. Buser, and suggested that buserite has the same crystal structure as synthetic "10Å manganite." Buserite was accepted as a mineral name by the Commission on New Minerals by a small majority (M. Fleischer, personal communication, 1974), and although it is listed in Hey and Embrey (1974), the name is absent from Fleischer's (1980) "Glossary of Mineral Species." Giovanoli and coworkers (1971, 1975) further contended from X-ray diffraction and electron

[1] Present address: Sandia National Laboratories, Albuquerque, New Mexico 87185.

0003–004X/83/0910–0972$02.00

microscopy measurements of synthetic manganese oxides that natural todorokites are a mixture of buserite and its decomposition products birnessite and manganite (γ-MnOOH). The Swiss group also recommended that todorokite should be discredited as a valid mineral (Giovanoli and Brutsch, 1979a, b; Giovanoli, 1980). However, recent experimental evidence verifying the integrity of todorokite includes results derived from infrared spectroscopy (Potter and Rossman, 1979), electron diffraction (Chukhrov *et al.*, 1978, 1979, 1981; Siegel, 1981), high resolution transmission electron microscopy (HRTEM) (Turner and Buseck, 1979, 1981, Turner *et al.*, 1982), and extended X-ray absorption fine structure (EXAFS) measurements (Crane, 1981) of manganese (IV) oxide minerals.

The conflicting viewpoints about todorokite have led us to critically evaluate experimental results and literature on buserite and todorokite. We summarize here evidence demonstrating that buserite and todorokite are distinct phases, describe recent observations of todorokite in marine manganese nodules, and discuss possible crystal structures and site occupancies of cations in the todorokite polymorphs. Finally, we recommend that todorokite takes precedence over buserite for the predominant 10Å phase in manganese nodules.

Survey of the crystal chemistry of todorokite and buserite

Todorokite

Todorokite occurs in a variety of terrestrial deposits. At the type locality in Japan, it is formed as an alteration product of inesite (Yoshimura, 1934). The economically important todorokite deposits of Cuba, such as Charco Redondo in Oriente Province, were formed syngenetically during the Eocene in foraminiferal oozes on the seafloor near fumerolic hot springs accompanying volcanic activity. Subsequent to lithification, some todorokite in the weathering zone has altered slightly to manganite, with more intense weathering yielding pyrolusite (Simons and Straczek, 1958; J. A. Straczek, personal communication, 1978). In other terrestrial localities, todorokite is reported to be of secondary origin (Frondel *et al.*, 1960; Larson, 1962). X-ray diffraction data show that considerable variations exist between relative intensities of comparable lines for different todorokite samples. Faulring (1962) attributed these large intensity variations, as well as the diffuseness of certain reflections, to preferred orientation of the fibrous crystallites of todorokite studied by her from Charco Redondo, Cuba. Thus, the most intense lines at 9.65Å and 4.82Å observed when X-rays are diffracted parallel to the fiber axis were weak or undetected for X-rays diffracted perpendicular to the crystallite axis. The most intense lines in the latter orientation occur at 2.42Å and 1.42Å. Faulring (1962) also suggested that manganite was topotactically intergrown with the Cuban todorokite, either forming simultaneously with todorokite, or resulting from its alteration. The latter observation was later cited as evidence by Giovanoli and coworkers (1971, 1975) for rejecting todorokite as a valid mineral.

Chemical analyses of todorokites in continental deposits (Straczek *et al.*, 1960; Frondel *et al.*, 1960; Nambu *et al.*, 1964) show that manganese is present in two oxidation states, and that Mn^{II}/Mn^{IV} ratios fall in the range 0.15–0.23. Significant amounts of Mg are also present, suggesting that relatively small divalent Mg^{2+} and Mn^{2+} ions are essential constituents of todorokite. The analyses show that Ca^{2+}, Na^{+} and to lesser extents K^{+}, Ba^{2+}, Ag^{+} (Radtke *et al.*, 1967) and Zn^{2+} (Larson, 1962), are also common constituents. Several chemical formulae have been proposed for todorokite, including (Ca,Na,K, Ba,Ag) (Mg, Mn^{2+},Zn) Mn_5^{4+} $O_{12} \cdot 3H_2O$ (Frondel *et al.*, 1960).

Most todorokites in hand specimen consist of fibrous aggregates of small acicular crystals, although platey morphologies have been observed. Electron micrographs (Straczek *et al.*, 1960; Hariya, 1961; Finkelmann *et al.*, 1974, Chukhrov *et al.*, 1978; Burns and Burns, 1979a) reveal that the crystals consist of narrow lathes or blades elongated along one axis (parallel to *b*) and frequently show two perfect cleavages parallel to (001) and (100).

A structural model for todorokite was inferred from its crystal morphology, cleavage properties and electron diffraction data (Burns and Burns, 1977b). It was noted that minerals of the hollandite–cryptomelane and psilomelane (romanèchite) groups also have fibrous or acicular habits and two perfect cleavages parallel to the fibre axis, as do a variety of synthetic Ti^{IV} oxides. Since these phases possess tunnel structures consisting of double and treble chains of edge-shared $[MnO_6]$ octahedra,[2] Burns and Burns (1977b) proposed that todorokite might also have a tunnel structure based on chains of multiple width edge-shared $[MnO_6]$ octahedra extending along its *b* axis. The correlation is borne out when comparisons are made between the unit cell parameters of todorokite, psilomelane, and hollandite-group minerals. Furthermore, todorokite and psilomelane both contain essential Mn^{2+} ions, and in psilomelane these divalent cations are located in specific positions in the triple chains of edge-shared octahedra. Burns and Burns suggested that Mn^{2+}, Mg^{2+}, Ni^{2+}, *etc.* might also be located in analogous sites in todorokite. The larger Ca^{2+}, Na^{+}, K^{+}, Ba^{2+}, *etc.* ions and H_2O molecules in todorokite were envisaged to occupy large tunnels in a psilomelane-like tektomanganate structure (Burns and Burns, 1979a). The site occupancies of cations in todorokite are discussed later.

Recent electron diffraction and high resolution trans-

[2] HRTEM measurements show [2×2] tunnels in hollandite-cryptomelane and [2×3] tunnels in psilomelane (romanèchite) (Turner and Buseck, 1979).

mission electron microscopy measurements of natural todorokites have confirmed the structural model for todorokite proposed by Burns and Burns (1977b, 1979a). Selected area electron diffraction (SAD) patterns of the Cuban todorokite with a = 9.75Å (Chukhrov *et al.*, 1978, 1979) revealed three less intense reflections (d = 9.75Å) corresponding to four sub-cells along the a^* axis between the strong reflections (d = 2.44Å) forming a pseudohexagonal net (Straczek *et al.*, 1960; V. M. Burns, unpublished data). This is in contrast to SAD patterns of synthetic buserite discussed later which contain only three sub-cells along the a^* axis (Giovanoli, 1980; V. M. Burns, unpublished data). HRTEM images of the Cuban todorokite (Turner and Buseck, 1981; Chukhrov *et al.*, 1978) revealed it to have a tunnel structure, in which [3×3] tunnels with dimensions 9.75Å × 9.59Å predominate (Turner and Buseck, 1981; Turner *et al.*, 1982). Chukhrov *et al.* (1978, 1979, 1981) studied todorokites from other localities, including a Pacific Ocean manganese nodule, and found SAD patterns having b (2.84Å) and c (9.59Å) parameters identical to the Cuban todorokite, but larger a parameters (14.6Å, 19.52Å and 24.38Å). Trilling intergrowths of these todorokites produce platey morphologies, while SAD patterns of the platelets reveal nets of hexagonal, triangular, and rhombic cells with four or five weaker reflections (d = 14.6Å or 24.38Å) between the strong reflections (d = 2.44Å) along the a^* axes (Chukhrov *et al.*, 1978; 1979; Burns and Burns, 1979a). Chukhrov *et al.* proposed that a family of todorokite species might exist having a unit cell parameters which are integral multiples of 4.88Å. Lattice image photographs of todorokite published by Chukhrov *et al.* (1978) also show evidence of structural disorder. In addition to the structure-types suggested by the variability of the a parameter, Chukhrov *et al.* found variations in the periodicity of the (100) planes. Thus, in addition to the main super-periodicity of todorokites producing a = 9.75Å and 14.6Å, defect layers with 7.32Å and 12.4Å were observed. These layers are multiples of 2.44Å, the height of the base (*i.e.*, dimensions of a [111] axis) of a MnO_6 octahedron.

Subsequent HRTEM images of todorokites from terrestrial deposits (Turner and Buseck, 1981) and from manganese nodules (Turner *et al.*, 1982; Turner and Buseck, 1982) revealed them to be intergrowths of tunnels of different widths. Although [3×3] dimensional tunnels predominate in todorokite, occasional tunnels with [3×2], [3×4], [3×5], [3×8] and higher dimensions were observed in crystals from both terrestrial and manganese nodule deposits.

Buserite

Buserite, which is assumed (Giovanoli *et al.*, 1971) to be equivalent to synthetic sodium manganese (II, III) manganate (IV) hydrate or "10Å manganite", is prepared by oxidation of fresh $Mn(OH)_2$ suspensions in cold aqueous NaOH solutions by molecular oxygen (Giovanoli *et al.*, 1970a). Synthetic buserite consists of elongated platelets which give an electron diffraction pattern with pseudohexagonal symmetry and weak superstructure reflections (d = 7.38Å) with a periodicity of three between major reflections (d = 2.46Å) in the basal (001) planes (Giovanoli, 1980). X-ray diffraction measurements (Giovanoli *et al.*, 1975; Giovanoli, 1980) reveal that the diagnostic intense lines representing basal plane separations occur in sodium buserite at 10.1–10.2 and 5.0–5.1Å; these distances are significantly larger than those measured in samples of marine manganese oxide deposits and in todorokite. A variety of buserite derivatives can be synthesized by cation exchange reactions (Wadsley, 1950a, b; Giovanoli *et al.*, 1975; Giovanoli and Arrhenius, 1983), and the Mg^{2+}, Cu^{2+}, Ni^{2+}, *etc.* derivatives have smaller basal plan spacings than the sodium-bearing parent buserite (Giovanoli, 1980). The transition metal derivatives appear to have greater thermal stabilities and to be more resistant to dehydration than the parent Na buserite (Giovanoli *et al.* 1975; Giovanoli and Arrhenius, 1983).

Sodium buserite readily decomposes when exposed to air. Drying over P_4O_{10} *in vacuo* leads to the formation of sodium birnessite, $Na_4Mn_{14}O_{27} \cdot 9H_2O$, which also has a platey morphology (Giovanoli *et al.*, 1970a; Giovanoli, 1980). The strongest basal plane X-ray diffraction lines then occur at 7.1 and 3.55Å. The electron diffraction patterns of the platelets again show pseudohexagonal symmetry and superstructure with only triple periodicity (Giovanoli *et al.*, 1970a; Giovanoli, 1980). The latter superstructure forms the basis for postulating a vacancy-ordered layered structure for birnessite (Giovanoli *et al.*, 1970a) based on the chalcophanite structure (Wadsley, 1955). The structure of chalcophanite, $Zn_2Mn_6O_{14} \cdot 6H_2O$, consists of layers of edge-shared $[MnO_6]$ octahedra and single sheets of water molecules between which the Zn^{2+} ions are located. The octahedral layer is only 6/7 filled by Mn^{4+}; that is, one out of every seven octahedral sites is vacant. The Zn^{2+} atoms occur above and below the vacancies in the octahedral layers, and the stacking sequence along the c axis is –O–Mn–O–Zn–H_2O–Zn–O–Mn–O–, so that consecutive $[MnO_6]$ layers are about 7.16Å apart. In the structure of sodium birnessite proposed by Giovanoli *et al.* (1970a), one out of every six octahedra is vacant, and Mn^{2+} and Mn^{3+} are suggested to lie above and below vacancies in the octahedral layer. The positions of the Na^+ ions are uncertain. Buserite is considered to have a similar layered structure, but additional OH^- ions and H_2O molecules are present so that the vacancy-ordered layers of $[MnO_6]$ octahedra are 9.6–10.1Å apart (Giovanoli, 1980). Recent intercalation studies of synthetic burserite (Paterson, 1981; Giovanoli and Arrhenius, 1983) correlate with its proposed layer structure.

When $Na_4Mn_{14}O_{27} \cdot 9H_2O$ is refluxed with dilute HNO_3 at 40°C, a sodium-free birnessite, $Mn_7O_{13} \cdot 5H_2O$, is obtained (Giovanoli *et al.*, 1970b) which again has a platey habit. The electron diffraction patterns of (001)

platelets show hexagonal symmetry, but streaks in the sub-cell are interpreted to be indicative of vacancy disordering in the $[MnO_6]$ octahedral layers. When $Mn_7O_{13} \cdot 5H_2O$ is subjected to careful reduction with cinnamyl alcohol, the platelets break down to extremely thin needles (Giovanoli *et al.*, 1971). These needles failed to give an X-ray diffraction pattern, but were believed to be γ-MnOOH (manganite). Giovanoli *et al.* (1971) proposed a mechanism for the topotactic transformation of $Mn_7O_{13} \cdot 5H_2O$ to "γ-MnOOH". They believed that the (001) layers of linked $[Mn^{IV}O_6]$ octahedra in birnessite correspond to chains of $[Mn^{III}(OH,O)_6]$ octahedra in the (010) plane of "γ-MnOOH," and that the [100] direction of birnessite became the needle axis (*c* axis) of the "γ-MnOOH" formed topotactically. The structural correlations suggested by Giovanoli *et al.* (1971) are shown in Figure 1, and are discussed later.

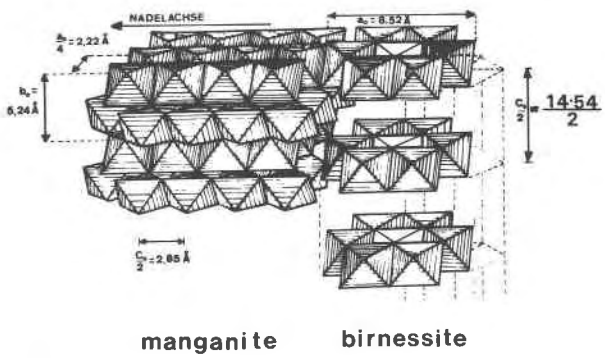

Fig. 1. Schematic structural diagrams relating the synthetic birnessite $Mn_7O_{13} \cdot 5H_2O$ phase (right) to its proposed topotactic transformation product manganite γ-MnOOH (left) [from Giovanoli *et al.*, 1971, Fig. 11].

These observations for buserite and its dehydration products formed the basis for Giovanoli and his coworkers (1971; 1975; 1979a,b; 1980) to propose that world-wide todorokite ores actually consist of buserite partly dehydrated to birnessite and partly reduced to needles of manganite (Giovanoli and Bürki, 1975). According to this view, the small amount of buserite in the ores accounts for the characteristic X-ray diffraction pattern, while a large amount of fibrous, nearly amorphous manganite accounts for the morphology. Apparently this "γ-MnOOH," which could not be detected by X-ray diffraction (due to its small crystallite size), is recognized on the basis of electron microscope observations of morphology. Thus, the argument against the integrity of todorokite as a mineral depends on the analogy with the topotactic decomposition of synthetic $Mn_7O_{13} \cdot 5H_2O$ (birnessite) to what could be unambiguously identified as γ-MnOOH on the basis of morphology and electron diffraction. Apparently, the morphology argument was considered stronger than the diffraction evidence, as the electron diffraction patterns observed for the hypothetical todorokite decay products do not match those of the experimental birnessite decay product.

Information from infrared spectroscopy

Some of the problems of identification and structural correlations for todorokite and buserite have been addressed by infrared spectroscopy (Potter and Rossman, 1979). In a study of numerous natural and synthetic manganese oxides, Potter and Rossman (1979) demonstrated that it is possible to distinguish between different $[MnO_6]$ structural linkages by their spectral profiles in the mid-infrared region. They have shown, for example, that the proposed layer structure of birnessite is supported by its infrared spectrum, and have confirmed the identity of natural birnessite with its synthetic analogues. The infrared spectra also show that synthetic buserite and birnessite have analogous structures, the shift from the 10Å to 7Å basal plane spacing in X-ray diffraction patterns being the result of water loss alone rather than to a structural rearrangement of the $[MnO_6]$ framework.

The infrared spectra of natural todorokites (Potter and Rossman, 1979) indicate that this mineral is not analogous to any synthetic phases, including buserite and its cation-exchanged derivatives, or to any decomposition products of buserite such as birnessite and manganite. Potter and Rossman suggested that the todorokite spectra are consistent with either a layer structure of linked $[MnO_6]$ octahedra containing vacancies, or a highly polymerized chain or tunnel structure with quadruple chains. Their hypothesis conforms with observations of the multidimensional tunnels found in subsequent studies of natural terrestrial and marine todorokites (Turner and Buseck, 1981, 1982; Turner *et al.*, 1982).

Discussion

The information derived from infrared spectroscopy, electron diffraction, and HRTEM measurements appear to demonstrate conclusively that todorokite and buserite are distinct phases having different linkages of edge-shared $[MnO_6]$ octahedra. Nevertheless, Giovanoli and coworkers (1971; 1975; 1979a, b; 1980; 1983) maintain that buserite is the primary phase and that todorokite is an assemblage of buserite and its breakdown products birnessite and manganite. However, close examination of the evidence presented by the Swiss group reveals apparent inconsistencies in interpretations of their data or questionable relevance of the results to geochemical processes.

First of all, there are the inferences from the laboratory studies that are not correlatable with sedimentary mineral formation. For example, the decomposition studies of synthetic $Mn_7O_{13} \cdot 5H_2O$ to the presumed manganite (γ-MnOOH) phase reported by the Swiss group were not performed on buserite, but on a sodium-free birnessite under conditions (reduction with cinnamyl alcohol) not found in nature. Also, the initial dehydration of Na buserite by drying over P_4O_{10} *in vacuo* and conversion of

Na birnessite to $Mn_7O_{13} \cdot 5H_2O$ by refluxing with dilute HNO_3 at 40°C are unlikely geochemical processes. Furthermore, the implication that todorokite in deep-sea manganese nodules represents buserite which has dehydrated *in situ* to birnessite is untenable. Second, the Swiss group did not prove that crystal morphology is more definitive than diffraction evidence for identifying manganite, but instead assumed that the fibrous pseudomorphs of decomposed $Mn_7O_{13} \cdot 5H_2O$ must be manganite, despite diffraction evidence to the contrary (see below). Third, although some todorokite ores in the weathering zone in Cuba have been slightly weathered to manganite and pyrolusite, there is no reason to believe that the fibrous habit of this material is due to a large component of non-diffracting manganite since fibrosity is an inherent property of all todorokites from other localities. Gram for gram, many todorokite ores give characteristic X-ray powder diffraction patterns (*not* containing manganite *d*-values) as intense or more intense than those of synthetic buserites. Such results are inexplicable if the ores consist of a mixture of non-diffracting manganite and undecomposed buserite.

A more rigorous examination of the evidence for the proposed birnessite→manganite topotactic relationship (Giovanoli and Stähli, 1970; Giovanoli, *et al.*, 1970a,b, 1971) reveals that the structural interpretation is incorrect. In the schematic structure of manganite (*e.g.*, Figure 11 in Giovanoli *et al.*, 1971), reproduced here in Figure 1, the authors inadvertently switched the *a* and *b* translations (with respect to the structure). In order to have the electron diffraction measurements actually agree with the true manganite structure (Buerger, 1936; Dachs, 1963), the idealized structure depicted in Figure 1 must be rotated 90° about the *c* axis. In this orientation, the planar triangular [111] surfaces of the $[Mn^{III}(OH,O)_6]$ octahedra in manganite no longer coincide with similar surfaces of the layers of $[Mn^{IV}O_6]$ octahedra in birnessite, so that the postulated topotaxy is much less evident. The structure correlation between manganite and birnessite suggested by Giovanoli *et al.* in Figure 1 has another inconsistency in that each row of $[MnO_6]$ octahedra in the birnessite structure is drawn to align with two rows of octahedra in the manganite structure one of which is devoid of Mn^{4+} ions, resulting in octahedra with unusual proportions. In addition, the structures sketched in Figure 1 reveal another problem (S. Turner, pers. comm., 1982) in that the spacing between the layers of birnessite is incorrect (relative to the manganite structure). They show a spacing of about 5Å instead of the true value of 7.27Å.

One of the consequences of mislabelling the axes of manganite in Figure 1 is that the indexing of electron diffraction patterns of the break down product of $Mn_7O_{13} \cdot 5H_2O$ purported to represent the a^*–c^* zero level of manganite (Giovanoli *et al.*, 1971, Figures 7 and 12; Giovanoli, 1980, Figure 15) does not satisfy criteria for the space group $B2_1/d$ determined for the manganite structure (Buerger, 1936). The diffraction pattern of the altered $Mn_7O_{13} \cdot 5H_2O$ phase (Giovanoli *et al.*, 1971; Giovanoli, 1980) does, however, roughly fit that expected for a (100) orientation for manganite (S. Turner, pers. comm., 1982). Apparently, previous experience with synthetic manganite (Giovanoli and Leuenberger, 1969) led to recognition of a manganite diffraction pattern but incorrect indexing of it.

In summary, although the topotactic relationship portrayed in Figure 1 has many flaws, the overall interpretation of the experimental work of the Swiss group may possibly be correct, and synthetic platey birnessite might break down to acicular manganite crystallites. However, it is difficult to follow the logic presented by Giovanoli and Bürki (1975) that fibrous todorokites naturally occuring in marine manganese nodules and in non-marine manganese ore deposits are mostly manganite. It becomes clear, though, that a critical step in their identification of manganite based on crystal morphology and electron diffraction evidence is ambiguous. Again, it is difficult to understand how the proposed buserite parent in marine manganese nodule deposits could have dehydrated to birnessite and decomposed to manganite *in situ* on the deep seafloor.

Finally, although past X-ray powder diffraction measurements of marine ferromanganese nodules and crusts have led to ambiguous identifications of todorokite or buserite ("10Å manganite"), it is significant that the more recent electron microscopy techniques have identified only todorokite in these seafloor deposits (Chukhrov *et al.*, 1978, 1979, 1981; Siegel, 1981; Turner and Buseck, 1982; Turner *et al.*, 1982). Buserite has yet to be positively identified in the natural environment. Such findings undermine the recommendation (Giovanoli *et al.*, 1971) that the "10Å phase" in manganese nodules be named buserite.

Crystal structure correlations

The recent HRTEM and infrared spectral measurements described earlier indicate that todorokites have tunnel structures analogous to hollandite and romanèchite (psilomelane). Turner and Buseck (1981) proposed a provisional nomenclature scheme for manganese (IV) oxide structures in which families are designated by the symbolism T(m,n), where T denotes a tunnel structure and m, n are the widths of infinite chains of edge-shared $[MnO_6]$ octahedra forming the walls of the tunnels. Thus, m = 1 defines the nsutite family in which T(1,1) and T(1,2) symbolize pyrolusite and ramsdellite, respectively. Intergrowths of these fundamental units, perhaps with higher dimensional tunnels T(1,3), T(1,4), *etc.* (Burns and Burns, 1980), characterize synthetic γ-MnO_2 and naturally-occurring nsutites (Turner and Buseck, 1983). Similarly, T(2,n) includes the cryptomelane-hollandite, T(2,2), and romanèchite (psilomelane), T(2,3), groups, together with the observed coherent intergrowths of T(2,4),—T(2,7) multidimensional tunnels found in fibrous manganese oxide minerals (Turner and Buseck, 1979). Turner

and Buseck (1981) suggested that the 7Å phyllomanganate birnessite phases represent the end-member T(2,∞) tunnel structure.

The todorokite family in the Turner and Buseck (1981) classification is represented by T(3,n) with T(3,3) the most common structure-type. The various coherent intergrowths in todorokites recognized by them (Turner and Buseck 1981, 1982; Turner *et al.*, 1982) and other workers (Chukhrov *et al.*, 1978, 1979, 1981) are designated T(3,2), T(3,3), T(3,4), T(3,5), T(3,6), T(3,7), *etc.*, while the end-member T(3,∞) is suggested to represent the phyllomanganate buserite phases.

Although this nomenclature summarizes the dimensions of the edge-shared [MnO_6] octahedral chains in todorokites, it does not define the structural details inside the tunnels. Some insight into the structure and crystal chemistry of todorokite can be deduced from correlations with the known crystal structure of psilomelane (Wadsley, 1953). The "floors" and "ceilings" of the [2×3] tunnels of psilomelane are formed by double chains of edge-shared [MnO_6] octahedra containing only Mn^{4+} ions in the M3 positions. The "walls", however, consist of triple chains of edge-shared octahedra (defining the psilomelane unit cell parameter a = 9.56Å), in which Mn^{4+} ions in the central M1 position are flanked by larger divalent cations in the M2 positions. In the todorokite [3×3] structure-type portrayed in Figure 2, the "walls" are suggested to be similar to those of psilomelane with divalent cations occupying outer M2 positions in the triple chains of edge-shared octahedra and Mn^{4+} ions located in the inner M1 positions (defining the unit cell parameter c = 9.59Å common to all structure-types of todorokite). The "floors" and "ceilings" in the most common todorokite [3×3] structure-type contain Mn^{4+} ions in M3 and M4 positions of triple chains of edge-shared [MnO_6] octahedra, giving rise to the unit cell parameter a = 9.75Å (Fig. 2). A (001) projection of the structure shown in Figure 2b provides another way of viewing the "floors" or "ceilings" of the todorokite structure. The triple chains of linked [MnO_6] run parallel to the b axis and are separated from adjacent triple chains by furrows of Mn^{4+} ion vacancies at the z = 0 level in the (001) plane. In the (001) projection (Figure 2b) divalent cations in M2 positions lie above and below the furrows at approximate levels z = 1/4 and 3/4.

The observations of different todorokite structure-types (Chukhrov *et al.*, 1978, 1979, 1981) and intergrowths of variable tunnel widths in todorokites (Turner and Buseck, 1981, 1982; Turner *et al.*, 1982) are depicted schematically in Figure 3. This figure shows an intergrowth of [3×3] and [3×5] tunnels, corresponding to the unit cell parameters a = 9.75Å and a = 14.6Å, respectively. Again, furrows of Mn^{4+} ion vacancies at the z = 0 level define the widths of the "ceilings" (or "floors") of the tunnels, as portrayed in Figure 3b. It becomes apparent from the (001) projections shown in Figures 2b and 3b that very wide tunnels attaining dimensions of [3×8] and

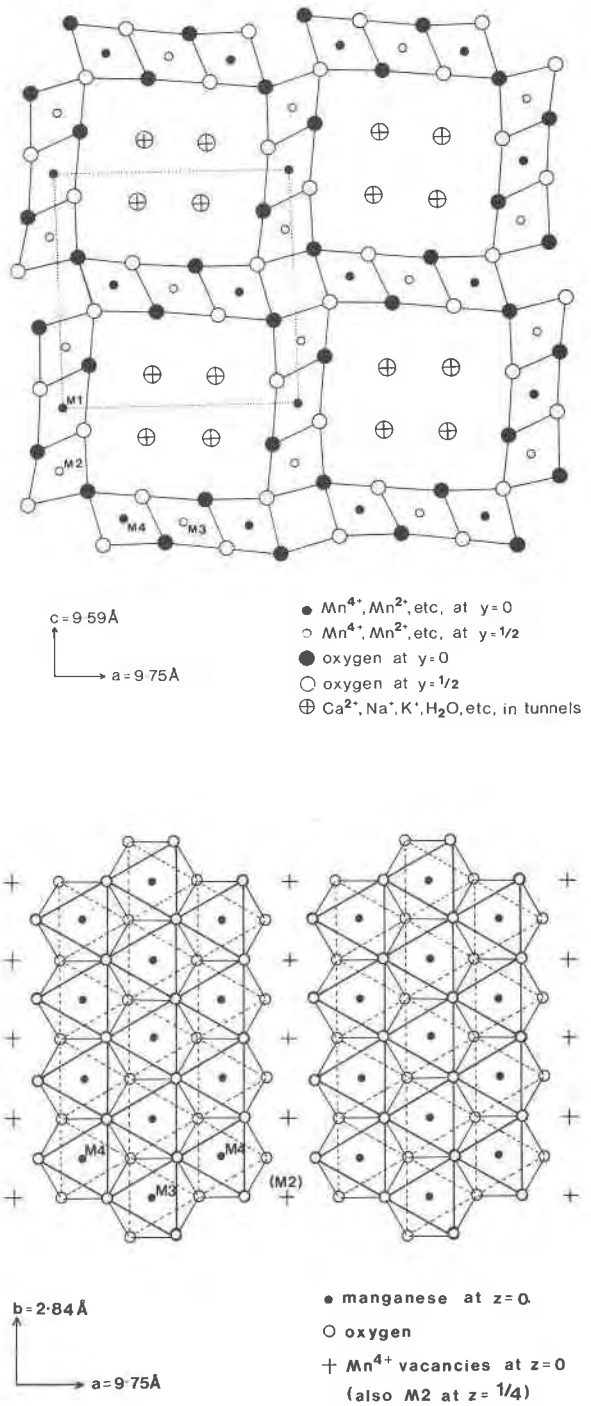

Fig. 2. Proposed crystal structure of todorokite. The diagram of Turner *et al.* (1982, Fig. 1) has been redrawn to resemble the psilomelane structure-type illustrated in Burns and Burns 1977b; Fig. 4) so as to highlight the linkages of [3×3] tunnels in todorokite (a) a (010) projection of the structure viewed down the [3×3] tunnels. (b) a (001) projection showing the triple chains of edge-shared [MnO_6] octahedra forming the "ceilings" or "floors" of the [3×3] tunnels. A (001) projection showing the triple chains constituting the "walls" is comparable.

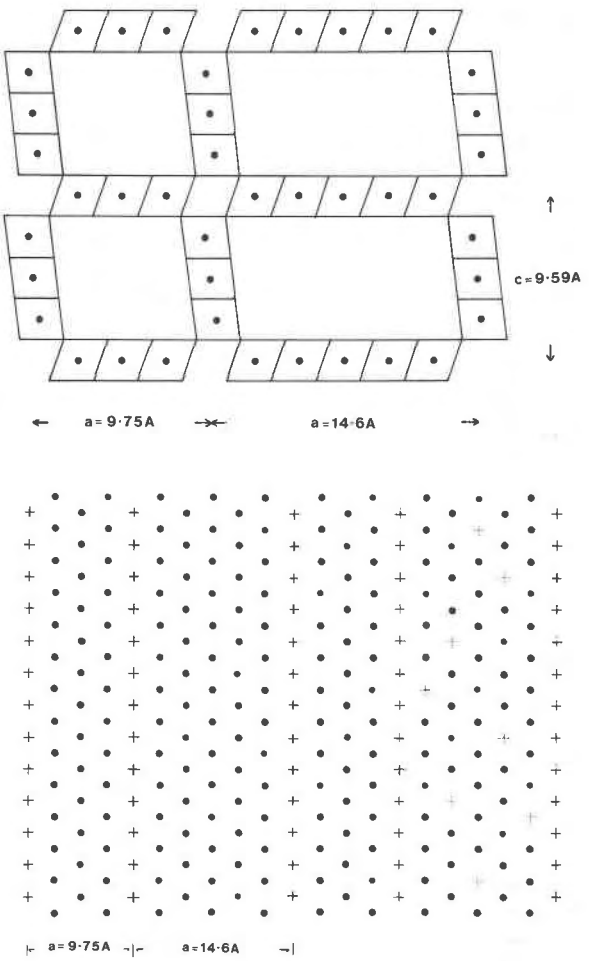

Fig. 3. Schematic intergrowth of [3×3] and [3×5] tunnels in todorokite. (a) a (010) projection viewed down the tunnels. (b) a (001) projection showing locations of Mn^{4+} cations in the "ceilings" of the tunnels. Some sporadic Mn^{4+} vacancies are shown to exist within the "ceilings" on the right of the diagram.

higher (Turner and Beseck, 1982) tend towards the [3×∞] layered structure postulated (Turner and Buseck, 1981) for buserite. Their predominance would provide grounds for expecting a buserite-like phase to occur naturally in marine manganese oxide deposits.

An important factor to be considered in the "ceilings" of the todorokite tunnels are cation vacancies within the bands of edge-shared [$Mn^{IV}O_6$] octahedra which probably become more prevalent the wider the "ceiling" dimension. As noted earlier, Mn^{4+} cation vacancies are essential features of chalcophanite (Wadsley, 1955), as well as numerous divalent cation (R^{2+})-bearing $R^{2+}{}_2Mn_3O_8$ phases (*e.g.*, Ostwald and Wampetich, 1967; Riou and Lecerf, 1975, 1977) and possibly synthetic birnessite (Giovanoli *et al.*, 1970a). In these phyllomanganates, the Mn^{4+} vacancies in sheets of edge-shared octahedra dictate their crystal chemistries because divalent cations are bonded in postions above and below the vacancies in the layered structures (Crane, 1981). We noted when discussing Figure 2b earlier that divalent cation-bearing M2 sites are located immediately above and below the furrows of Mn^{4+} ion vacancies in the (001) planes of todorokite. Similar Mn^{4+} ion vacancies may also be present within the "ceilings" of todorokite, particularly where multiple-width edge-shared [MnO_6] domains exist. Examples are sketched in Figure 3b. These cation vacancies not only may nucleate faults, kinks, and twinning observed in HRTEM micrographs of todorokite fibers (Turner *et al.*, 1982), but they also would influence the crystal chemistry and site occupancies of the tunnel interiors. As a result, three types of atomic substitution might contribute to the crystal chemistry of todorokite. First, substitution of Mn^{4+} cations by cations of similar ionic radii (0.53–0.55Å) in the "ceilings", such as low-spin Co^{3+} ions (Burns, 1976). Second, substitution of divalent Mn^{2+} ions in the "walls" by Mg^{2+}, Ni^{2+}, Cu^{2+}, Zn^{2+} and other cations having ionic radii in the range 0.65–0.80Å, and third, constituents of the tunnels. The latter would consist of a variety of large cations (K^+, Ba^{2+}, Ag^+, Na^+, Ca^{2+}, Pb^{2+}), H_2O molecules, and smaller hyrated cations adjacent to Mn^{4+} vacancies in the "ceilings."

The cation site occupancies of todorokites and buserites proposed here also account for relative stabilities toward oxidation. Todorokite and synthetic buserite are both destabilized by the presence of substantial Mn^{2+} ions in the structures, which are vulnerable to oxidation. Thus, Mn^{2+}-todorokites are oxidized to vernadite (Chukhrov *et al.*, 1978, 1979), while synthetic buserites are oxidized (accompanied by dehydration) to birnessites. However, replacement of Mn^{2+} by Mg^{2+}, Zn^{2+}, Ni^{2+}, and Cu^{2+}, which are not susceptible to oxidation, stabilize both todorokite and buserite.

Although detailed crystal structure refinements of these cryptocrystalline manganese oxides are urgently required to establish the precise similarities and differences between todorokites and buserites, it is apparent that currently available evidence demonstrates that they are distinct phases.

Conclusions and recommendations

Critical examination of the published literature on todorokites and buserites leads to the following conclusions.

(1) Naturally occurring todorokites and synthetic buserites are crystallographically distinct phases.

(2) Stability relationships linking the mineral todorokite to synthetic buserite and its suggested break down products birnessite and γ-MnOOH were deduced from phases prepared and degraded in the laboratory under conditions not encountered in geochemical processes.

(3) The validity of todorokite as a distinct mineral group has been demonstrated and a family of todorokite structure-types exists possessing multi-dimensional tunnels

symbolized by T(3,n), where n, the dimension of the "ceilings," is most commonly 3 (triple chains of edge-shared [MnO_6] octahedra). However, n may range from 2 to 7 or higher. With this terminology, $n \rightarrow \infty$ may represent the buserite group.

(4) Todorokite, not "10Å manganite" or buserite, is the abundant Mn(IV) oxide 10Å phase occurring in maganiferous concretions and crusts including seafloor ferromanganese nodule deposits.

Acknowledgments

We are indebted to several people for helpful discussions, including Drs. G. Arrhenius, C. Bowser, P. Buseck, S. Crane, G. Faulring, M. Fleischer, C. Frondel, M. Hey, J. Hunter, H. Jaffe, R. McKenzie, U. Marvin, G. Mellors, P. Moore, J. Murray, R. Potter, G. Rossman, J. Straczek, and W. Zwicker. We thank Dr. G. Arrhenius for sending us a preprint of his paper with R. Giovanoli. Dr. S. Turner provided an extremely constructive review of the manuscript. Research on the mineralogy of manganese nodules was supported by the National Science Foundation (grant number OCE-7827495) and the I.C. Sample Office (U.S. Electrochemical Society, Cleveland Section).

Note Added

Two recent publications support the conclusions reached in this paper. First, todorokite is now acknowledged by Perseil and Giovanoli (1982) to have several features in common with the 10Å phase in marine manganese nodules. This finding originates from XRD, TEM, SEM and EMP measurements of todorokite from the eastern Pyrenees. Second, further evidence for the tunnel structure of todorokite is described by Arrhenius and Tsai (1981), who suggest that todorokite forms diagenetically from buserite in marine manganiferous deposits.

References

Arrhenius, G. (1963) Pelagic sediments. In M. N. Hill, Ed., The Sea, p. 655–727, Vol. 3. Interscience Publication, New York.

Arrhenius, G. O. and Tsai, A. G. (1981) Structure, phase transformation, and prebiotic catalysis in marine manganate minerals. Scripps Institution of Oceanography Reference Series 81-28, 1–19.

Buerger, M. J. (1936) The symmetry and crystal structure of manganite, Mn(OH)O. Zeitschrift für Kristallographie, 95, 163–174.

Burns, R. G. and Burns V. M. (1977a) Mineralogy of manganese nodules. In G. P. Glasby, Ed., Marine Manganese Deposits, p. 185–148. Elsevier Publishing Company, New York.

Burns, R. G. and Burns, V. M. (1977b) The mineralogy and crystal chemistry of deep-sea manganese nodules, a polymetallic resource of the twenty-first century. In Mineralogy: Towards the 21st Century (Centenary Volume, Mineralogical Society, London, p. 49–67) Philosophical Transactions of the Royal Society of London, A286, 283–301.

Burns, R. G. and Burns, V. M. (1979a) Manganese oxides. In R. G. Burns, Ed., Marine Minerals, p. 1–46. Reviews of Mineralogy, Vol. 6. Mineralogical Society of America, Washington, D. C.

Burns, R. G. and Burns, V. M. (1980) Recent structural data for manganese (IV) oxides. In B. Schumm, Jr., H. M. Joseph, and A. Kozawa, Eds., Manganese Dioxide Symposium, Vol. 2, p. 97–112. Electrochemical Society Publication, Cleveland.

Burns, V. M. and Burns, R. G. (1978) Post-depositional metal-enrichment processes in manganese nodules from the equatorial Pacific. Earth and Planetary Science Letters, 39, 341–348.

Burns, V. M. and Burns, R. G. (1979b) Observations of processes leading to the uptake of transition metals in manganese nodules. In C. Lalou, Ed., La Genèse des Nodules de Manganèse, no. 289, p. 305–315. Colloquium International du Centre National de la Recherche Scientifique.

Buser, W. (1959) The nature of the iron and manganese compounds in manganese nodules. In M. Sears, Ed., International Oceanography Congress, Abstracts, p. 962–963.

Chukhrov, F. V., Gorshkov, A. I., and Sivtsov, A. V. (1981) A new structural variety of todorokite. Izvestia Akademia Nauk, S.S.S.R., Series Geology, 5, 88–91.

Chukhrov, F. V., Gorshkov, A. I., Sivtsov, A. V., and Berezovskaya, V. V. (1978) Structural varieties of todorokite. Izvestia Akademia Nauk, S.S.S.R., Series Geology, 12, 86–95.

Chukhrov, F. V., Gorshkov, A. I., Sivtsov, A. V., and Beresovskaya, V. V. (1979) New data on natural todorokites. Nature, 278, 631–632.

Crane, S. E. (1981) Structural Chemistry of the Marine Manganate Minerals. Ph.D. Thesis, University of California, San Diego.

Cronan, D. S. (1980) Underwater Minerals. Academic Press, New York.

Dachs, H. (1963) Neutronen-und Röntgenuntersuchungen am Manganite, γ-MnOOH. Zeitschrift für Kristallographie, 118, 303–326.

Faulring, G. M. (1962) A study of Cuban todorokite. In M. Mueller, Ed., Advances in X-ray Analysis, Vol. 5, p. 117–126.

Feitknecht, W., and Marti, W. (1945) Über die oxidation von mangan (II) hydroxide mit molekularem sauerstoff. Über manganite und künstlichen braunstein. Helvetica Chimica Acta, 28, 129–148 and 149–157.

Finkelmann, R. B., Evans, H. T., Jr., and Matzko, J. J. (1974) Manganese minerals in geodes from Chihuahua, Mexico. Mineralogical Magazine, 39, 549–558.

Fleischer, M. (1980) Glossary of Mineral Species 1980. Mineralogical Record, Arizona.

Frondel, C., Marvin, U. B., and Ito, J. (1960) New occurrences of todorokite. American Mineralogist, 45, 1167–1173.

Giovanoli, R. (1980) On natural and synthetic manganese nodules. In I. M. Varentsov, and G. Grasselly, Eds., Geology and Geochemistry of Manganese, vol. 1, p. 159–202, E. Schweizerbart'sche Verlagsbuchhandlung, Stuttgart.

Giovanoli, R. and Arrhenius, G. (1983) Structural chemistry of marine manganese and iron minerals and synthetic model compounds. In P. Halbach, Ed., Marine Mineral Deposits: New Research Results and Economic Prospects. Gluckauf, Essen, West Germany.

Giovanoli, R., and Brütsch, R. (1979a) Über Oxidhydroxide des Mn(IV) mit Schichtengitter. 5. Mitteilung: Stochiometrie, Austrauschverhalten und die Rolle bei der Bildung von Tiefsee-Mangankonkretionen. Chimia, 33, 372–376.

Giovanoli, R., and Brütsch, R. (1979b) L'échange des ions de transition par le manganate-10Å et le manganate-7Å. In C. Lalou, Ed., La Genèse des Nodules de Manganèse, no. 289, Coloquium International du Centre National de la Recherche Scientifique no. 289, 305–315.

Giovanoli, R., and Bürki, P. (1975) Comparison of X-ray evidence of marine manganese nodules and non-marine manganese ore deposits. Chimia, 29, 114–117.

Giovanoli, R. and Leuenberger, U. (1969) Über die oxydation von Manganoxidhydroxid. Helvitica Chimica Acta, 52, 2333–2347.

Giovanoli, R., and Stähli, E. (1970) Oxide und Oxidhydroxide des dreiund vierwertigen Mangans. Chimia, 24, 49–61.

Giovanoli, R., Bürki, P., Giuffredi, M., and Stumm, W. (1975) Layer structured manganese oxide hydroxides. IV: The buserite groups; structure stabilization by transition elements. Chimia, 29, 110–113.

Giovanoli, R., Feitknecht, W., and Fischer, F. (1971) Über Oxidhydroxide des vierwertigen Mangans mit Schichtengitter. 3. Mitteilung: Reduktion von Mangan (III)–manganat (IV) mit Zimtalkohol. Helvitica Chimica Acta, 54, 1112–1124.

Giovanoli, R., Stähli, E., and Feitknecht, W. (1970a) Über Oxidhydroxide des vierwertigen Mangans mit Schichtengitter. 1. Mitteilung: Natrium-mangan (II,III) manganat (IV). Helvitica Chimica Acta, 53, 209–220.

Giovanoli, R., Stähli, E., and Feitknecht, W. (1970b) Über Oxidhydroxide des vierwertigen Mangans mit Schichtengitter. 2. Mitteilung: Mangan (III)-manganat (IV). Helvitica Chimica Acta, 53, 453–464.

Glasby, G. P. (1977) Marine Manganese Deposits. Elsevier Publishing Company, New York.

Hariya, Y. (1961) Mineralogical studies on todorokite and birnessite from the Todoroki mine, Hokkaido. Japanese Journal of the Association of Mineralogists, Petrologists, and Economic Geologists, 45, 219–230.

Hewitt, D. F., Fleischer, M., and Conklin, N. (1963) Deposits of the manganese oxides: supplement. Economic Geology, 58, 1–51.

Hey, M. H. and Embrey, P. G. (1974) Twenty-eighth list of new mineral names. Mineralogical Magazine, 39, 903–932.

Larson, L. T. (1962) Zinc-bearing todorokite from Philipsburg, Montana. American Mineralogist, 47, 59–66.

Levinson, A. A. (1960) Second occurrence of todorokite. American Mineralogist. 45, 802–807.

Nambu, M., Okada, K., and Tanida, K. (1964) Chemical composition of todorokite. Japanese Journal of the Association of Mineralogists, Petrologists, and Economic Geologists, 51, 30–38.

Paterson, E. (1981) Intercalation of synthetic buserite by dodecyclammonium chloride. American Mineralogist, 66, 424–427.

Perseil, E-A. and Giovanoli, R. (1982) Étude comparative de la todorokite d'Ambollas (Pyrénées Orientales), des manganates à 10Å recontrés dans les nodules polymétalliques des océans et des products de synthèse. Compte Rendu Academic Science de Paris, 294, 199–202.

Potter, R. M. and Rossman, G. R. (1979) The tetravalent manganese oxides: identification, hydration, and structural relationships by infrared spectroscopy. American Mineralogist, 64, 1199–1218.

Radtke, A. S., Taylor, C. M., and Hewett, D. R. (1967) Aurorite, argentian todorokite, and hydrous silver-bearing lead manganese oxide. Economic Geology, 62, 186–206.

Siegel, M. D. (1981) Studies of the Mineralogy, Chemical Composition, Textures and Distribution of Manganese Nodules at a Site in the North Equatorial Pacific Ocean. Ph.D. Thesis, Harvard University, Cambridge.

Simons, F. S., and Straczek, J. A. (1958) Geology of the manganese deposits of Cuba. U. S. Geological Society Bulletin, 1057, 1–283.

Straczek, J. A., Horen, A., Ross, M., and Warshaw, C. M. (1960) Studies of the manganese oxides. IV. Todorokite. American Mineralogist, 45, 1174–1184.

Turner, S. and Buseck, P. R. (1979) Manganese oxide tunnel structures and their intergrowths, Science, 203, 456–458.

Turner, S. and Buseck, P. R. (1981) Todorokites: a new family of naturally occurring manganese oxides. Science, 212, 1024–1027.

Turner, S. and Buseck, P. R. (1982) HRTEM and EDS of tops and bottoms of some Ni-bearing manganese nodules. EOS, 63, 1010.

Turner, S. and Buseck, P. R. (1983) Defects in nsutite (γ-MnO_2), a dry-cell battery cathode. Nature, in press.

Turner, S., Siegel, M. D., and Buseck, P. R. (1982) Structural features of todorokite intergrowths in manganese nodules. Science, 296, 841–842.

Wadsley, A. D. (1950a) A hydrous manganese oxide with exchange properties. Journal of the American Chemical Society, 72, 1782–1784.

Wadsley, A. D. (1950b) Synthesis of some hydrated manganese minerals. American Mineralogist, 35, 458–499.

Wadsley, A. D. (1953) The crystal structure of psilomelane, $(Ba,H_2O)_2Mn_5O_{10}$. Acta Crystallographica, 6, 165, 172.

Wadsley, A. D. (1955) The crystal structure of chalcophanite, $ZnMn_3O_7 \cdot 3H_2O$. Acta Crystallographica, 8, 165–172.

Yoshimura, T. (1934) Todorokite, a new manganese mineral from the Todsoroki Mine, Hokkaido, Japan. Journal of the Faculty of Science, Hokkaido University, Sapporo, Series 4, Vol. 2, 289–297.

Manuscript received, December 21, 1981;
accepted for publication, February 22, 1983.